HHS Public Access

Author manuscript

Clin Neurophysiol. Author manuscript; available in PMC 2021 February 03.

Published in final edited form as:

Clin Neurophysiol. 2019 April ; 130(4): 454–468. doi:10.1016/j.clinph.2019.01.010.

Differences between flexion and extension synergy-driven coupling at the elbow, wrist, and fingers of individuals with chronic hemiparetic stroke

Laura Miller McPherson[a,b,c,d], **Julius P.A. Dewald**[a,b,e,*]

[a]Department of Physical Therapy and Human Movement Sciences, Feinberg School of Medicine, Northwestern University, Chicago, IL, USA

[b]Department of Biomedical Engineering, McCormick School of Engineering, Northwestern University, Evanston, IL, USA

[c]Department of Physical Therapy, Nicole Wertheim College of Nursing and Health Sciences, Florida International University, Miami, FL, USA

[d]Department of Biomedical Engineering, College of Engineering and Computing, Florida International University, Miami, FL, USA

[e]Department of Physical Medicine and Rehabilitation, Feinberg School of Medicine, Northwestern University, Chicago, IL, USA

Abstract

Objective: The flexion and extension synergies were quantified at the paretic elbow, forearm, wrist, and finger joints within the same group of participants for the first time. Differences in synergy expression at each of the four joints were examined, as were the ways these differences varied across the joints.

Methods: Twelve post-stroke individuals with chronic moderate-to-severe hemiparesis and six age-matched controls participated. Participants generated isometric shoulder abduction (SABD) and shoulder adduction (SADD) at four submaximal levels to progressively elicit the flexion and extension synergies, respectively. Isometric joint torques and EMG were recorded from shoulder, elbow, forearm (radioulnar), wrist, and finger joints and muscles.

Results: SABD elicited strong wrist and finger flexion torque that increased with shoulder torque level. SADD produced primarily wrist and finger flexion torque, but magnitudes at the wrist were less than during SABD. Findings contrasted with those at the elbow and forearm, where torques and EMG generated due to SABD and SADD were opposite in direction.

*Corresponding author at: 645 N. Michigan Ave, Suite 1100, Chicago, IL 60611, USA. Fax: +1 312 908 0741. j-dewald@northwestern.edu (J.P.A. Dewald).

Appendix A. Supplementary material

Supplementary data to this article can be found online at https://doi.org/10.1016/j.clinph.2019.01.010.

Conflict of interest statement

None of the authors have potential conflicts of interest to be disclosed.

Conclusions: Flexion and extension synergy expression are more similar at the hand than at the shoulder and elbow. Specific bulbospinal pathways that may underlie flexion and extension synergy expression are discussed.

Significance: Whole-limb behavior must be considered when examining paretic hand function in moderately-to-severely impaired individuals.

Keywords

Stroke; Upper extremity; Flexion synergy; Extension synergy; Hand; Rehabilitation; Reticulospinal; Vestibulospinal; Bulbospinal

1. Introduction

Individuals with chronic hemiparetic motor impairment following stroke, particularly those who are moderately-to-severely impaired, have a limited ability to selectively and independently control proximal and distal upper limb joints for purposeful activity (Beer et al., 2004; Sukal et al., 2007; Miller and Dewald, 2012; Lan et al., 2017a; McPherson et al., 2018a; McPherson et al., 2018c). Movement of the upper limb is constrained to two stereotypical multi-joint movement patterns, the flexion and extension synergies, that simultaneously couple activation of shoulder, elbow, wrist, and finger muscles. Clinical observations describe the flexion synergy as shoulder abduction (SABD) coupled with elbow flexion, supination, and wrist and finger flexion. The extension synergy is described as shoulder adduction (SADD) coupled with elbow extension, pronation, and variable postures at the hand, possibly including wrist extension and finger flexion (Twitchell, 1951; Brunnstrom, 1970; Radomski and Latham, 2008).

Experimental work quantifying these synergy patterns has been extensive. Variables ranging from surface EMG to single joint torque to whole arm kinematics have been studied within a variety of paradigms that elicit the synergies through SABD and SADD torque generation (including single- and/or multi-joint tasks and isometric and/or dynamic upper limb activation; see, e.g., Dewald et al. (1995), Dewald and Beer (2001), Ellis et al. (2007), Miller and Dewald (2012), Miller et al. (2014), Ellis et al. (2016b)). Results have provided insight into the effects of the synergies on functional use of the arm (Ellis et al., 2008; Seo et al., 2009; Ellis et al., 2017; Lan et al., 2017a; McPherson et al., 2018c) and the potential neural mechanisms that may underlie the emergence of the synergies (Ellis et al., 2012; Owen et al., 2017; McPherson et al., 2018a; McPherson et al., 2018c). Findings have directly motivated the development of targeted rehabilitation interventions and neuroprostheses (Ellis et al., 2009; Makowski et al., 2013, 2014, 2015; Ellis et al., 2016a; Lan et al., 2017b; Wilkins et al., 2017; Ellis et al., 2018).

However, the vast majority of this research has focused on coupling between the shoulder and elbow, even though for individuals with chronic hemiparetic motor impairment following stroke, the most profound deficits of the upper limb joints are typically found at the hand (Colebatch and Gandevia, 1989; Turton et al., 1996; Miller and Dewald, 2012). Paretic hand dysfunction has been studied extensively in isolation from the rest of the upper limb (reviewed briefly in Miller and Dewald (2012)), but concurrent shoulder and elbow

activation further degrades hand function due to expression of the flexion synergy (Seo et al., 2009; Miller and Dewald, 2012; Lan et al., 2017a).

We have recently quantified aspects of flexion synergy expression at the wrist and fingers (Miller and Dewald, 2012; Lan et al., 2017a), but quantification of the extension synergy at these distal joints has not been explored. In addition, forearm pronation and supination, integral to many functional tasks involving the hand, have not been quantified in this context. This study will quantify the expression of both the flexion and extension synergies at the forearm, wrist, and finger joints for the first time. Further, it will replicate previous quantification of the synergies at the elbow in order to allow a comprehensive understanding of how the synergies manifest at proximal and distal joints within the same sample of research participants.

Specifically, the objectives of this study were: (1) to comprehensively quantify the flexion synergy at the forearm, wrist and fingers by extending our previous work (Miller and Dewald, 2012; Lan et al., 2017a), (2) to quantify the expression of the extension synergy at these joints for the first time, (3) to determine how flexion synergy expression differs from extension synergy expression at the elbow, forearm, wrist, and finger joints, and (4) to compare how these differences vary across the joints.

To accomplish these objectives, we elicited the synergies in individuals post-stroke via isometric torque generation tasks in SABD and SADD (to elicit the flexion and extension synergies, respectively). The tasks were completed at four different SABD and SADD torque levels because previous work has demonstrated that synergy expression is proportional to the level of torque generated in these directions (e.g., Dewald and Beer (2001), Miller and Dewald (2012), McPherson et al. (2018c)). We quantified synergy expression in terms of isometric joint torque measurements from the elbow, forearm, wrist, and fingers, as well as surface EMG from nine elbow, wrist, and finger muscles. While the flexion and extension synergies are inherently paretic limb phenomena, the experimental conditions designed to elicit them in the paretic limb were also applied to non-paretic and control limbs for comparative purposes.

2. Methods

2.1. Participants

Individuals with chronic hemiparesis due to a stroke at least 1year prior were recruited through the Clinical Neuroscience Research Registry, hosted by Northwestern University and the Shirley Ryan Ability Lab. Participation required sufficient passive range of motion at the shoulder, elbow, wrist, and fingers for the arm to be secured comfortably to the testing setup. A physical therapist conducted a clinical exam for potential participants. Acceptable clinical motor deficits for inclusion in the study were those consistent with cortical or sub-cortical lesions (e.g., unilateral hemiparesis with non-cerebellar, non-brainstem clinical signs). Specific lesion locations were obtained for 9 of the 12 participants from either the participant's medical records or, when available, a computed tomography scan and/or a T1-weighted magnetic resonance imaging scan. Lesion locations were determined from scans

that had not been interpreted by a radiologist by research personnel with training in neuroanatomy.

Exclusion resulted from of any one of the following four conditions: (1) an upper extremity Fugl-Meyer Motor Assessment (FMA) (Fugl-Meyer et al., 1975) score less than 9 (indicating near paralysis) or greater than 44 (indicating mild impairment); (2) a score on the hand portion of the Chedoke-McMaster Stroke Assessment (CMSAh) (Gowland et al., 1995) greater than 5 (indicating mild impairment); (3) significant impairment of vision or upper extremity tactile somatosensation; (4) the current use of botox in the paretic upper extremity. Twelve individuals post-stroke met all inclusion criteria and completed the study (three females, nine males; mean age: 59.0 years; mean time post-stroke 10.3 years; range: 3.5–26.6years; Table 1). Participants exhibited severe to moderate arm and hand motor impairment, based on FMA scores (range 13–31, mean 22.7) and CMSAh scores (range 2–4, mean 3.0), respectively. Six participants with no known neurological injury (four males, two females; mean age 60.6 years) formed the control group and were included for comparison with the non-paretic arm of participants with stroke. Written informed consent was obtained from all participants prior to inclusion in the study, which was approved by the Institutional Review Board of Northwestern University.

2.2. Experimental setup and data collection

The experimental protocol was carried out in a testing device capable of measuring isometric shoulder, elbow, forearm (i.e., proximal and distal radio-ulnar (Neumann et al., 2017)), wrist, and finger (i.e., metacarpophalangeal) joint torques simultaneously (Fig. 1). Participants were seated in an experimental chair (Biodex, Inc.) with shoulder/waist straps to prevent shoulder girdle and trunk motion. A fiberglass cast was made for the tested forearm to rigidly interface the arm with a six degree-of-freedom load cell (JR3, model 45E15A) through a Delrin ring. The wrist and fingers were placed in a custom Wrist and Finger Torque Sensor (WFTS) (Stienen et al., 2011). The arm was positioned in 75° shoulder abduction, 40° horizontal adduction, 90° elbow flexion, 15° pronation, and 0° wrist flexion/extension.

Fingers from the paretic arm were positioned at 15° finger flexion to accommodate range of motion restrictions. Fingers from the non-paretic and control arms were positioned at 0° finger flexion/extension because at 15° of finger flexion, the increased strength of these two groups slightly deformed the WFTS attachment bracket and interfered with the measurement of maximum voluntary isometric torques. A computer monitor displayed real-time visual feedback of joint torque data.

Electromyography (EMG) was recorded using active differential surface electrodes with a 1-cm interelectrode distance (16-channel Bagnoli EMG System; Delsys, Inc.; 1000× gain, 20–450 Hz band-pass) placed over the following muscles, according to the land-marks described by Perotto and Delagi (1994): anterior deltoid, sternocostal head of the pectoralis major, biceps brachii, lateral head of the triceps brachii, extrinsic wrist and finger flexors (flexor carpi radialis (FCR), flexor digitorum profundus (FDP)), an intrinsic finger flexor (first dorsal interosseous (FDI)), extrinsic wrist and wrist/finger extensors (extensor carpi radialis (ECR), extensor digitorum communis (EDC)), and two thumb muscles (flexor pollicis brevis

(FPB) and extensor pollicis longus (EPL)). A signal conditioner (Frequency Devices, Model 9064) filtered (8th-order Butter-worth low-pass filter, 500 Hz) and amplified EMG and wrist and finger torque data before digitization at a sampling frequency of 1 kHz.

2.3. Experimental protocol

Each participant's maximum voluntary torques (MVTs) and corresponding maximum voluntary muscle contractions (MVC) were measured during isometric torque generation in the following directions: SABD, SADD, elbow flexion, elbow extension, wrist flexion, wrist extension, finger flexion, finger extension, thumb flexion (for MVC only) and thumb extension (for MVC only). In addition, MVTs in pronation and supination directions were measured for 5 of the participants with stroke (both arms) and all of the control participants. Order of performance of the MVT directions was randomized, and trials within a direction were repeated until three trials with peak torque within 85% of the maximum torque value were obtained. If the last trial produced the largest peak torque, an additional trial was collected. Participants were given vigorous verbal encouragement throughout MVT trials.

Visual feedback of torque performance for MVT trials was provided for the intended torque direction only. A large circle appeared on the computer screen that formed a speedometer-like gauge with a moving needle that reflected real-time torque magnitude. This was provided for all torque directions except for wrist extension and finger extension while testing the paretic limb. Because most participants with stroke had little to no voluntary wrist and finger extension on the paretic side, efforts to produce these movements often resulted in flexion (a phenomenon previously described by Kamper et al. (2003) and Miller and Dewald (2012)). Therefore, no visual feedback was given for these directions to ensure participants' maximal effort.

For submaximal torque generation trials, participants completed blocks of three trials at each of 17, 33, and 50% of SABD MVT and SADD MVT, with the order of conditions randomized for each participant. Real-time visual feedback of SABD/SADD torque was displayed on the computer screen as a green circle that moved up from the center of the screen when SABD torque was produced and down when SADD torque was produced. A red circle served as a stationary target for the desired torque level (17, 33, 50% MVT) and direction (SABD or SADD) for a given set of trials. Participants moved the green circle up or down (for SABD or SADD, respectively) into the red circle to achieve the desired torque direction and level and held it for 3–5 s before relaxing. Torques from other shoulder degrees of freedom and other joints were not shown. Participants were instructed to focus on activating the shoulder and not to intervene at the distal joints.

2.4. Data processing

All data analysis was performed using custom MATLAB software. A Jacobian-based algorithm was used to convert forces and moments collected from the six degree-of-freedom load cell attached at the distal forearm into shoulder and elbow joint torques. Torque and full-wave rectified EMG data were smoothed using an acausal one-sided moving average filter with a window length of 250 ms, were baseline corrected so that any passive stiffness or muscle tone at rest would not factor into subsequent analyses, and were normalized to the

largest value obtained during the entire experiment. This normalization value was chosen instead of the maximum value during a maximal voluntary contraction because paretic limb voluntary wrist and finger torque and EMG values were often very small in comparison to values generated during other MVT directions, resulting in inflated values if normalized in this manner.

Maximal torque in the primary (i.e., intended) direction was determined for each MVT trial. Secondary torques (i.e., those at joints other than the primary joint) at the time of maximal primary torque were determined, as were EMG values at 50 ms preceding the maximal value, to account for an estimate of the electromechanical delay associated with excitation-contraction coupling of skeletal muscle (Cavanagh and Komi, 1979).

For each sub-maximal SABD or SADD trial, maximal normalized secondary torque values generated while participants held the targeted SABD or SADD torque were identified, as were the EMG values at 50 ms preceding. For each participant, values across trials per MVT direction and submaximal condition were averaged prior to including in subsequent group analyses.

In assessing EMG data from individual muscles related to Objective 3, a surprising pattern of findings in the wrist and finger EMG data emerged when comparing results from SABD vs. SADD torque generation. Three distinct patterns of behavior were observed among group mean values of the seven muscles: (1) *virtually identical* EMG for SABD and SADD, (2) *less* EMG with SABD than SADD, or (3) *greater* EMG with SABD then SADD. Because the patterns were so striking, new variables were created by grouping muscles into categories associated with the three patterns of behavior above. EMG data from FCR and FDP exhibited pattern 1 and were averaged to create a common EMG value for the ‘‘extrinsic wrist/finger flexor muscle group.” Similarly, EMG data from EDC, EPL, FDI, and FPB exhibited pattern 2 and were averaged to create a common EMG value for the ‘‘wrist/finger extensor and intrinsic hand muscle group.” Lastly, ECR was the only muscle to exhibit pattern 3, therefore, EMG data were not altered for subsequent analyses. To be consistent with presentation of results for Objective 3, and for clarity in presentation of results, wrist and finger EMG data are presented in these three groups for all Objectives throughout the Results section.

2.5. Data and statistical analyses

For all statistical analyses, $p < 0.05$ was used to determine statistical significance. Cases where p-values were greater than 0.05 but less than 0.10 are presented.

2.5.1. Objectives 1 and 2—To address Objective 1, quantification of the flexion synergy at the paretic forearm, wrist, and fingers, data from SABD torque generation conditions were compared with those from the non-paretic limb. Between-limb analyses of the data were performed using nine separate 2 × 4 repeated measures ANOVAs to test the effect of limb (paretic, non-paretic) and torque load (17, 33, 50, and 100% MVT) on each of the nine dependent variables (elbow, forearm, wrist, and finger torque, as well as EMG for each muscle/muscle group: biceps, triceps, and the three wrist and finger muscle groups listed in Section 2.4). The effects relevant to this study were the main effect of limb and the

limb-by-torque load interaction. Therefore, results of the main effect of torque load are not presented, nor are they presented for subsequent ANOVAs in the following Objectives. When relevant, post-hoc t-tests on the limb-by-torque interaction were calculated to determine between-limb differences at each torque load, using a Bonferroni correction for multiple comparisons.

To address Objective 2, quantification of the extension synergy at the paretic forearm, wrist, and fingers, data from SADD torque generation conditions were compared with those from the non-paretic limb using the same analyses as for Objective 1.

2.5.2. Objective 3—To address Objective 3, determining differences between flexion and extension synergy expression at each joint, within-limb comparisons were made between SABD and SADD torque generation conditions. For the paretic limb and for the non-paretic limb, nine separate 2 × 4 repeated measures ANOVAs were conducted to determine the effect of shoulder direction (SABD, SADD) and torque load on each of the nine dependent variables (elbow, forearm, wrist, and finger torque; EMG for each muscle/muscle group). The ANOVA effects relevant to this study were the main effect of shoulder direction and the shoulder direction by torque load interaction. Therefore, results of the main effect of torque load are not presented, nor are they presented for subsequent ANOVAs.

To assist with interpretation of elbow torque values, the relative level of biceps and triceps EMG within each arm was examined using a biceps-triceps co-contraction index calculated as: $(biceps_{EMG} - triceps_{EMG})/(biceps_{EMG} + triceps_{EMG})$. A value of −1 on this index indicates triceps but no biceps EMG, a value of 0 indicates equal EMG for the two muscles, and a value of 1 indicates biceps but no triceps EMG. Statistical significance of the biceps-triceps co-contraction indices relative to a value of zero (indicating parity in biceps and triceps EMG) was evaluated for each shoulder direction (combined across torque levels) using a one-sample t-test. A Bonferroni correction was used for the four total comparisons (SABD and SADD for the paretic and non-paretic arms).

2.5.3. Objective 4—To address Objective 4, comparing how differences in flexion and extension synergy expression vary across the elbow, forearm, wrist, and finger joints, several analyses were used. First, we determined whether there was a difference in the magnitude of secondary torque generation across the joints, and whether such differences varied with SABD and SADD. A 2 × 4 repeated measures ANOVA was conducted to determine the effect of shoulder direction (SABD, SADD) and joint (elbow, forearm, wrist, finger) on the magnitude of secondary torque (averaged across torque loads). This analysis did not factor in the direction of secondary torque generation, only the magnitude.

Second, we compared the magnitude of the change in *direction* of secondary torque generation between SABD and SADD torque generation across joints. This analysis took into account the direction of secondary torque generation as follows. Secondary torques were expressed on a continuum of 100% MVT to −100% MVT for agonist/antagonist directions (i.e., shoulder abduction(+)/adduction(−), elbow flexion(+)/extension (−), forearm supination(+)/pronation(−), wrist flexion(+)/extension(−), and finger flexion(+)/extension(−)). The torque values plotted in Figs. 2–4 reflect this convention. The magnitude

of the change in direction was calculated as the absolute value of the difference in secondary torque between SABD and SADD torque generation directions. The maximum value of this metric is 200% MVT (which, for example, is the value for the shoulder when comparing 100% MVT SABD torque generation and 100% MVT SADD torque generation). A 5 × 4 repeated measures ANOVA was conducted to determine the effect of joint (shoulder, elbow, forearm, wrist, finger) and torque load on the magnitude of the change in direction of secondary torque. Post-hoc pairwise comparisons on all combinations of the main effect of joint were calculated using Tukey's method to correct for multiple comparisons.

Third, we compared whether increasing descending motor drive via increasing shoulder torque load resulted in preferential activation of flexor or extensor muscles for the elbow and wrist/finger joints. For this analysis, EMG data were grouped as follows. Group mean elbow and wrist/finger EMG data were separated into flexors (biceps EMG for the elbow and extrinsic flexor EMG (FCR, FDP) for the wrist/fingers) and extensors (triceps for the elbow and extrinsic extensors (ECR, EDC) for the wrist/fingers). EMG from both the SABD and SADD conditions were averaged together for the flexor and extensor groups for the elbow and for the wrist/finger joints. For this analysis, only the extrinsic wrist/finger flexor muscles were included and not the intrinsic hand muscles, because the extrinsic muscles have clear roles as flexors and extensors, whereas the intrinsic hand muscles have more multi-planar function. For comparison of flexor and extensor EMG, separate 2 × 4 repeated measures ANOVAs (muscle type (flexor, extensor) × torque load) were conducted for the elbow and for the extrinsic wrist/finger muscles for both the paretic and non-paretic limbs.

2.5.4. Missing cases—In this study, 960 EMG recordings were attempted (80 possible per participant (2 arms × 2 shoulder directions × 4 torque loads × 5 muscles/muscle groups) × 12 participants). Some missing cases occurred due to poor signal quality or placement of electrodes interfering with the forearm-load cell interface, but overall they were limited in number. There were two types of missing cases.

First, for some participants, usable EMG data for EPL or FPB were not available for all 8 conditions for a given arm (2 shoulder directions × 4 torque loads). This occurred for 4 participants in the paretic arm and 4 different participants in the non-paretic arm. These cases reduced the total number of available EMG recordings from 960 to 896. There were no instances in which data for both EPL and FPB were missing in the same participant. As described in Section 2.5.2, EMG values for the wrist/finger extensor/intrinsic hand muscle group were calculated as the average of the values for EPL, FPB, EDC, and FDI within each participant for each task. Therefore, for the participants for whom all EPL or FPB data were missing, calculation of EMG for the wrist/finger extensor/intrinsic hand muscle group was based on the average of EMG values from the other three available muscles.

Second, there were five individuals for whom EMG was missing for only one or two out of 80 possible recordings (nine missing values in total over all participants). In these cases, the individual's EMG value was imputed from the average of the other 11 subjects in the same experimental task. Imputation was used in these cases because the repeated measures ANOVAs used in the study require a complete set of data. It is unlikely that such limited imputation (only 1% of cases–9/896 × 100) led to biased results, particularly because

ANOVAs computed with data from fewer participants with complete datasets revealed similar results to those presented here.

2.5.5. Role of control group—Because changes in motor function of the non-paretic upper limb have been demonstrated during some tasks (Miller and Dewald, 2012; Bowden et al., 2014; McNulty et al., 2014), we included a group of individuals without central nervous system injury for comparison with non-paretic limb data. However, in this study, results from non-paretic and control groups were highly similar with no meaningful variations. Therefore, the control data were not included in statistical analyses; however, torque data from the control group is shown graphically in Fig. 3 for visual comparison.

3. Results

Fig. 2 shows single trial data from the paretic limb of one participant during a 50% SABD MVT trial (top panel) and a 50% SADD MVT trial (bottom panel). The pattern of joint torque and EMG data during SABD and SADD torque generation in these trials reflects the general pattern of the group mean data, presented in detail in the following sections. Compared with the majority of participants, the participant whose data are shown in Fig. 2 demonstrated a greater decrease in wrist and finger flexion torques from SABD to SADD torque generation.

3.1. Objective 1: Quantification of the flexion synergy

3.1.1. Torque results for SABD torque generation—Fig. 3 shows group mean torque data for the shoulder, elbow, forearm, wrist, and finger joints in the paretic group (A), the non-paretic group (B), and the control group (C). The left panels display the joint torques generated when the primary torque direction was SABD, and the right panels display joint torques generated when the primary torque direction was SADD. The leftmost sets of bars in each plot illustrate that participants were able to accurately generate the target levels of SABD torque (left panel) and SADD torque (right panel). The remaining clusters of bars show the group mean normalized secondary torques (i.e., elbow flexion/extension, forearm pronation/supination, wrist flexion/extension, and finger flexion/extension).

As a result of SABD torque generation, substantial secondary torques were generated by the paretic limb at all joints, in elbow flexion, forearm supination, and wrist and finger flexion directions (Fig. 3A, left panel). In the non-paretic and control limbs, there were appreciable secondary torques only at the elbow (in flexion) and at the forearm (in supination) (Fig. 3B and C, left panel).

The middle panel of Table 2 summarizes results of separate 2 × 4 repeated measures ANOVAs examining the main effect of limb (paretic, non-paretic) and the interaction effect of limb-by-torque load (17, 33, 50, 100% MVT) on elbow, forearm, wrist, and finger torque during SABD. Paretic limb secondary torques for the elbow, wrist, and finger were significantly higher on average across torque load than those of the non-paretic limb (main effect of limb); however, for the forearm, they were not significantly different ($p = 0.70$). Similarly, for each joint except the forearm ($p = 0.45$), there was a significant limb-by-torque

load interaction whereby the paretic values became progressively larger than the non-paretic values with increasing torque load.

3.1.2. EMG results for SABD torque generation—Fig. 4 shows the paretic and non-paretic limb group mean normalized EMG values for the biceps, triceps, and the three wrist/finger muscle groups during SABD torque generation (solid lines). Note that the elbow, wrist, and finger torque data from the left panels of Fig. 3A and B are displayed again at the bottom of Fig. 4 to assist with interpretation of EMG data. The middle panel of Table 3 summarizes results of separate 2 × 4 repeated measures ANOVAs examining the main effect of limb (paretic, non-paretic) and interaction effect of limb-by-torque load (17, 33, 50, 100% MVT) on biceps, triceps, extrinsic wrist/finger flexors, wrist/finger extensors/intrinsic hand muscles, and ECR during SABD torque generation.

Paretic EMG values (solid black lines in Fig. 4) were higher than the non-paretic EMG values (solid light purple lines in Fig. 4) (significant main effects of limb) for all muscles/muscle groups except for triceps ($p = 0.43$). The increased paretic EMG for these muscles/muscle groups was substantial. On average across participants, the ratio of paretic to non-paretic mean EMG was 2.79 ± 0.74 (mean ± SEM) for the biceps, 4.83 ± 1.08 for the extrinsic wrist/finger flexors, 3.42 ± 0.80 for the wrist/finger extensors/intrinsic hand muscles, and 3.83 ± 0.80 for the ECR. (Data were excluded from the calculation of these ratios if the non-paretic EMG value was <2%, to prevent abnormally high values; 8 of 48 possible values were excluded.)

With increasing torque load, EMG values for the paretic and non-paretic limbs diverged (significant limb-by-torque load interactions) for all muscles except triceps ($p = 0.29$), with paretic values increasing more rapidly across torque load. In the 100% SABD MVT condition, group mean EMG values in the paretic limb ranged from 15.6% (triceps) to 65.3% (biceps) and those in the non-paretic limb ranged from 8% (wrist/finger extensors and intrinsic hand muscles) to 34% (biceps).

3.2. Objective 2: Quantification of the extension synergy

3.2.1. Torque results for SADD torque generation—As a result of SADD torque generation, substantial secondary torques were generated by the paretic limb at all joints in elbow extension, forearm pronation, and wrist and finger flexion directions (Fig. 3A, right panel). In the non-paretic and control limbs, there were appreciable secondary torques only at the forearm (in pronation) (Fig. 3B and C, right panel).

The right panel of Table 2 summarizes results of separate 2 × 4 repeated measures ANOVAs examining the main effect of limb and the interaction effect of limb-by-torque load on elbow, forearm, wrist, and finger torque during SADD torque generation. As with SABD torque generation in Objective 1, paretic limb secondary torques for the elbow, wrist, and finger joints were significantly higher than those of the non-paretic limb (main effect of limb). For the forearm, paretic secondary torques were significantly greater than those of the non-paretic limb only at the $p < 0.10$ level ($p = 0.072$). For all joints except the elbow, there was a significant limb-by-torque load interaction, whereby the difference between paretic and non-paretic values increased with torque load. For the forearm, post-hoc t-tests

performed on the significant limb-by-torque load interaction to explore the nature of the non-significant main effect of limb revealed that paretic forearm pronation torque values were significantly greater in magnitude than non-paretic values only at the 100% MVT level (68.0% vs.18.0% MVT, $p < 0.0001$) but not at the 17, 33, or 50% MVT levels.

3.2.2. EMG results for SADD torque generation—The right panel of Table 3 summarizes results of separate 2 × 4 repeated measures ANOVAs examining the main effect of limb and the interaction effect of limb-by-torque load on each EMG variable during SADD torque generation. Paretic EMG values (dashed black lines in Fig. 4) were higher than non-paretic values (dashed light purple lines in Fig. 4) (significant main effects of limb) for extrinsic wrist/finger flexors and wrist/finger extensors/intrinsic hand muscles but not biceps ($p = 0.28$) or ECR ($p = 0.95$). EMG values for triceps were significant at the $p < 0.10$ level ($p = 0.08$).

The group mean ratio of paretic to non-paretic EMG for SADD was 3.29 ± 0.64 for the extrinsic wrist/finger flexors, 4.04 ± 0.91 for the wrist/finger extensors/intrinsic hand muscles, and 2.12 ± 0.49 for the triceps. (As with SABD, data were excluded from the calculation of these ratios if the non-paretic EMG value was <2%, to prevent abnormally high values; 7 of 36 possible values were excluded.)

With increasing torque load, EMG values for the paretic and non-paretic limbs diverged for the extrinsic wrist/finger flexors, wrist/finger extensors/intrinsic hand muscles, and the triceps (significant limb-by-torque load interactions), with paretic values increasing more rapidly across torque load. For triceps, post-hoc t-tests performed on the significant limb-by-torque load interaction to explore the nature of the non-significant main effect of limb revealed that paretic triceps EMG values were significantly greater than non-paretic values at only the 100% MVT level (45% vs. 24.5% MVC, $p = 0.0002$).

The interaction for ECR EMG was significant at the $p < 0.10$ level ($p = 0.06$), but pattern of the two groups over torque level did not demonstrate divergence of paretic and non-paretic values with increasing torque load. The paretic biceps EMG during SADD was similar to the non-paretic biceps EMG during both SABD and SADD conditions, and the shoulder direction-by-torque load was not significant ($p = 0.26$). Maximal group mean EMG values (occurring at 100% MVT) in the paretic limb ranged from 27.8% (biceps) to 51.0% (extrinsic wrist/finger flexors) and those in the non-paretic limb ranged from 8% (wrist/finger extensors and intrinsic hand muscles) to 24.5% (triceps).

3.3. Objective 3: Differences in flexion vs. extension synergy at each joint

For brevity, non-paretic results are summarized here and not discussed in detail in the following sub-sections. For torque data, results of the 2 × 4 shoulder direction by torque load ANOVA are shown for each joint in the right panel of Table 4. Findings are consistent with visual inspection of Fig. 3B, namely, that there were significant effects of shoulder direction at elbow and forearm joints but at not wrist and finger joints (which exhibited no secondary torques). For EMG data shown in Fig. 4, there were no significant ANOVA effects for any of the muscles.

3.3.1. Differences in paretic torque during SABD vs. SADD—For both the paretic elbow and forearm joints, secondary torques in response to production of SABD and SADD torque were opposite in direction, with elbow flexion and forearm supination resulting from SABD torque and elbow extension and forearm pronation resulting from SADD torque (Fig. 3A). As shown in the middle panel of Table 4, the 2 × 4 repeated measures ANOVAs (shoulder direction (SABD, SADD) × torque load (17, 35, 50, 100%)) conducted for the elbow and the forearm joints resulted in significant main effects of shoulder direction and significant shoulder direction-by-torque load interactions ($p < 0.0001$ for each effect and joint).

For both the wrist and fingers, secondary torques in response to production of SABD and SADD torque were in the same direction (flexion) (Fig. 3A). As shown in the middle panel of Table 4, the main effect of shoulder direction was significant only at the 0.10 level for both wrist torque ($p = 0.06$) and finger torque ($p = 0.09$). There was, however, a significant shoulder direction-by-torque load interaction for wrist torque ($p = 0.02$), whereby the difference between paretic and non-paretic values increased with torque load, but for not finger torque ($p = 0.22$).

Because the main effect of shoulder direction was significant only at the 0.10 level for both wrist and finger torque, post-hoc t-tests were performed on the significant shoulder direction-by-torque load interaction. They revealed that wrist torque values were significantly greater during SABD than during SADD at the 33% ($p = 0.03$), 50% ($p < 0.0001$), and 100% ($p = 0.0002$) MVT levels, but not the 17% level ($p > 0.99$). Similarly, finger torque values were significantly greater during SABD than during SADD at the 33% (p=0.03), 50% (p=0.0003), and 100% (p=0.008) MVT levels, but not the 17% level (p=0.73). In addition, the difference in wrist and finger flexion torque between SABD to SADD was examined for each individual participant. During generation of SABD torque, all 12 participants produced flexion torque at both the wrist and fingers. During generation of SADD torque, however, the direction of the wrist and finger torque varied. Seven of the 12 participants demonstrated greater wrist and finger flexion torque as a result of SABD compared with SADD torque generation, the pattern that is reflected in the group means. For three of these seven participants, the decrease in wrist flexion torque with SADD torque generation was so great that very slight wrist extension resulted. The two remaining participants (out of 12) demonstrated the opposite pattern, with SABD torque generation resulting in less flexion torque than SADD torque generation. A re-analysis of the 2 × 4 repeated measures ANOVAs presented in Table 4 without these two participants resulted in a significant main effect of limb, for which torque during SABD was significantly higher than that during SADD (for wrist ($p = 0.001$) and finger torque ($p = 0.004$), respectively).

3.3.2. Differences in paretic EMG during SABD vs. SADD—Table 5 summarizes results of 2 × 4 (shoulder direction × torque load) repeated measures ANOVAs for each EMG variable. For paretic biceps and triceps EMG, data complemented the elbow torque results, as the biceps was recruited more during SABD than SADD torque generation (main effect of shoulder direction) and triceps displayed the opposite pattern (main effect of shoulder direction). There was a significant shoulder direction-by-torque load interaction for

each elbow muscle, reflecting that the difference in EMG between shoulder directions increased with increasing shoulder torque load.

For the paretic limb, the biceps-triceps co-contraction indices for each shoulder direction were significantly different than zero. The mean ± SEM biceps-triceps co-contraction index was + 54.4 ± 4.3% ($p < 0.0004$) for SABD and −29.7 ± 6.8% ($p < 0.0004$) for paretic SADD, indicating that there was greater biceps than triceps EMG during SABD and the opposite pattern during SABD. This pattern was not present for the non-paretic limb, for which the biceps-triceps co-contraction index not significant for any of the conditions, with mean ± SEM values of 7.8 ± 8.8% ($p = 0.81$) and −1.7 ± 8.5% ($p = 0.99$) and for SABD and SADD, respectively.

As shown in Fig. 4, SABD and SADD torque generation resulted in EMG values for the paretic extrinsic wrist/finger flexor group that were virtually identical at each torque load (left column, middle row). There was no significant effect of shoulder direction ($p = 0.64$) or shoulder direction-by-torque load ($p = 0.82$) on paretic extrinsic wrist/finger flexor EMG. In contrast, EMG values for the wrist/finger extensors/intrinsic hand muscle group were significantly less with SABD than SADD and increasingly so with torque level (significant main effect of shoulder direction and significant shoulder direction-by-torque load interaction).

EMG values for ECR were significantly *higher* with SABD than SADD and increasingly so with torque level (significant main effect of shoulder direction and shoulder torque-by-shoulder direction interaction). It could be proposed that this finding resulted from cross-talk in the surface EMG values from nearby muscles activated during SABD (most likely the elbow flexor brachioradialis). To evaluate this possibility, we analyzed data from a separate experiment in the paretic limb of two of the participants in this study using intramuscular EMG recordings (bipolar fine-wire electrodes with 5-mm recording surfaces; data was amplified (Nor-axon fine-wire pre-amplifiers) and acquired at 10 kHz (Alligator amplifier, SCS-816)). After placement of intramuscular wires into the ECR muscle was confirmed using electrical stimulation through the recording wires, the same SABD and SADD torque generation conditions were conducted. The surface EMG results were confirmed: in both participants, the ECR EMG was substantially higher during SABD than during SADD (mean across torque loads: 34.8% vs. 4.1% MVC for SABD and SADD, respectively, for the first participant and 16.3% vs. 4.2% MVC for the second participant).

Combined across shoulder directions and torque loads, the extrinsic wrist/finger flexor muscle group had the highest EMG values, averaging 25.0 ± 6.0% MVC (mean ± SEM) compared with 16.0 ± 5.0% from the wrist/finger extensors/intrinsic hand muscles and 16.4 ± 5.7% from the ECR.

3.4. Objective 4: Comparison of flexion and extension synergy expression among joints

3.4.1. Differences in the magnitude of secondary torques—As shown in Fig. 3A, the magnitude of secondary torques generated by the paretic elbow, forearm, wrist, and fingers is similar across joints for both SABD and SADD conditions. In the 2 × 4 shoulder direction × joint repeated measures ANOVA, there was no significant difference in

secondary torque among the joints (main effect of joint, $p = 0.90$). There was, however, a significant increase in overall secondary torques during SABD compared with SADD (main effect of shoulder direction, $p = 0.015$). SABD torque generation elicited secondary torques that were 10% MVT greater in magnitude than those for SADD torque generation (38.8 ± 1.1% MVT vs. 28.3 ± 2.1% MVT (mean ± SEM)). The shoulder direction-by-joint interaction was not statistically significant ($p = 0.14$).

3.4.2. Differences in the magnitude of change in direction of secondary torques—As discussed in Section 3.3.1, data from the paretic limb exhibited striking differences among joints in terms of the *direction* of secondary torques that results from SABD vs. SADD torque generation (Fig. 3A). Fig. 5 shows the magnitude of change in torque direction due to SABD vs. SADD torque generation for each joint, calculated as described in Section 2.5.3. The magnitude of change in torque values for the shoulder are predictably close to double the torque load targets of 17, 33, 50, and 100% MVT, given that shoulder torque generation at these levels was a controlled independent variable.

The 5 × 4 repeated measures ANOVA (joint by torque load) conducted on the magnitude of change in torque direction values showed a significant main effect of joint ($p < 0.0001$) and a significant joint-by-torque load interaction ($p < 0.0001$). Post-hoc tests on the main effect of joint revealed that all pair-wise comparisons were significantly different (p-values ranging from <0.0001 to 0.0005) except for wrist vs. finger ($p = 0.67$) and elbow vs. forearm joints ($p = 0.99$). Values for the shoulder were significantly higher than those of each other joints, and values for the elbow and forearm joints were significantly higher than those for the wrist and fingers.

3.4.3. Effect of increasing torque load on elbow and wrist/finger flexors and extensors—Fig. 6 shows flexor and extensor EMG values at each torque load (averaged across shoulder directions) for paretic elbow (left) and extrinsic wrist/finger (right) muscle groups. For paretic elbow muscles, a 2 × 4 repeated measures ANOVA (muscle type × torque load) revealed not only that flexor (biceps) EMG was significantly greater than extensor (triceps) EMG on average across torque levels (20.5% vs. 15.0%; main effect of muscle type, $p = 0.03$), but also that it increased at a significantly faster rate across increasing torque load levels (significant muscle type-by-torque load interaction, $p = 0.0002$, mean difference in EMG at each torque load: 5.7%). Results for the paretic extrinsic wrist/finger muscles were similar, but the differences between muscle types was more pronounced. The flexor (FCR, FDP) EMG was significantly greater than extensor (ECR, EDC) EMG (25.8% vs. 15.0%; main effect of muscle type, $p < 0.0001$), and it increased at a significantly faster rate across increasing torque load levels, particularly between 17 and 50% MVT (muscle type-by-torque load interaction, $p = 0.005$, mean difference in EMG at each torque load: 10.8%).

For the non-paretic limb, flexor and extensor EMG were virtually identical for both the elbow and wrist/finger muscles (data not shown graphically). There were no significant effects of muscle type or muscle type-by-torque load) ($p = 0.36$, $p = 0.40$ for elbow; $p = 0.34$, $p = 0.60$ for wrist/fingers).

4. Discussion

This study provides the first comprehensive quantitative summary of progressive flexion and extension synergy expression at all major upper limb joints. Using isometric joint torque measurements from the shoulder, elbow, forearm, wrist, and finger joints and surface EMG from elbow, wrist, and finger muscles, the expression of each synergy was quantified at each joint, and the difference in flexion vs. extension synergy expression was compared among the joints. Our results demonstrated for the first time that extension synergy expression throughout the limb, like flexion synergy expression, progressively increases with descending drive requirements.

4.1. Objective 1: Quantification of the flexion synergy

In the paretic arm, secondary torques during SABD were in directions consistent with clinical descriptions and with the results of studies that quantified flexion synergy expression at the elbow joint alone (Dewald and Beer, 2001; Ellis et al., 2005; Ellis et al., 2007), with wrist and finger measurements combined (Miller and Dewald, 2012), and with fingers alone (Lan et al., 2017a). Here, we demonstrated that SABD torque generation led to secondary flexion torque at both the wrist and the fingers in the paretic arm of all participants.

The current study also quantified expression of the flexion synergy at the forearm joint for the first time. We demonstrated that SABD torque generation elicits forearm supination, also consistent with the clinical description of the flexion synergy. However, paretic values were not different than those of the non-paretic arm. Interestingly, supination as a result of SABD torque generation was found even in participants who exhibited forearm pronation postures at rest or when moving the upper limb outside of the testing device. This finding suggests that passive tissue restrictions or resting hypertonicity in the pronator muscles in these participants may mask aspects of underlying neural activation during movement, reinforcing the well-known understanding that these factors compete for resulting limb movement.

Mean paretic EMG was increased in all wrist/finger muscles and selectively in the biceps, compared to the non-paretic arm. Mean triceps EMG did not differ between groups. Although SABD also resulted in secondary elbow flexion torque in the non-paretic arm (albeit significantly less than the paretic arm), mean biceps and triceps values were virtually identical in the non-paretic arm. This finding suggests that these muscles were co-contracting for typical postural stabilization rather than as part of the pathological flexion synergy. Indeed, as a biarticular muscle, the long head of the biceps provides stability to the glenohumeral joint during shoulder abduction (Neumann et al., 2017), and triceps activation would offset some of the resulting elbow flexion torque. Similarly, the secondary forearm supination torque that was generated during SABD may be a consequence of biceps activation that was unopposed by forearm pronators.

4.2. Objective 2: Quantification of the extension synergy

In the paretic arm, secondary torques of elbow extension and forearm pronation during SADD were consistent with the clinical description of the extension synergy, as were

secondary torques at the wrist and fingers. There was some variability in the direction of secondary wrist torque during SADD, but the majority of participants produced wrist torque in the flexion direction. The wrist extension torque that was observed in 3 of 12 participants was small and coincident with finger flexion torque, rendering the overall effect unlikely to provide functional benefits. In a more mildly-impaired cohort, there may be greater and more prevalent secondary wrist extension torque during SADD. For the fingers, all participants generated flexion torque.

EMG results from the paretic arm during SADD were consistent with secondary torque findings. In the non-paretic arm, small values of EMG were present in all muscle groups, but they likely represent typical co-contraction for postural stabilization, given that secondary torques for the elbow, wrist, and finger joints were negligible.

4.3. Objective 3: Differences in flexion vs. extension synergy at each joint

The manifestation of the synergies at the paretic wrist and fingers contrasts with that at the shoulder, elbow, and forearm joints. At more proximal joints, the flexion and extension synergies resulted in torques that are strongly opposite in direction (SABD vs. SADD, elbow flexion vs. extension, supination vs. pronation). The change in elbow torque direction can be explained by the selective increases in biceps and triceps activation that occurred for the flexion and extension synergies, respectively. In contrast with proximal joints, at the wrist and fingers, both synergies resulted overwhelmingly in flexion torque. Nevertheless, differences between the synergies were still found at these joints. The magnitude offlexion torque for both the wrist and the fingers was smaller for the extension synergy at 33, 50, and 100% MVT. Additionally, differences between the synergies were found in EMG data from wrist and/or finger muscles. They demonstrated one of three conspicuous patterns: (1) virtually identical EMG as part of both synergies, (2) increased EMG as part of the extension synergy, or (3) increased EMG as part of the flexion synergy.

Surprisingly, mean EMG values of the extrinsic wrist/finger flexor muscle group (FCR and FDP) were virtually identical during SABD and SADD torque generation. Given that individuals with post-stroke hemiparesis typically have more strength, increased resting tone, and better volitional control of their wrist and finger flexors compared with their extensors, it might have been expected that changes in activation of the primary flexor muscles, FCR and FDP, would underlie the changes in wrist and finger flexion torque. However, this was not the case, as values were strikingly similar during SABD and SADD. The high level of EMG from these muscles, combined with their greater torque generation capacity relative to wrist/finger extensors (both pre- and post-stroke) (Gonzalez et al., 1997; Kamper et al., 2006), likely explains the persistence of wrist and finger flexion torque as part of both flexion and extension synergies.

The wrist/finger extensor/intrinsic hand muscle group (EDC, EPL, FDI, FPB) exhibited less EMG during SABD compared with SADD, demonstrating that these muscles are recruited more strongly as part of the extension synergy than the flexion synergy. Given that both EDC and EPL generate extension torque at the wrist, the increase in activation of these muscles during SADD could explain the observed decrease in wrist flexion torque. In fact, based on musculoskeletal modeling, the EDC generates wrist extension torque of

comparable magnitude with the ECR, with the EPL contributing a smaller amount (Gonzalez et al., 1997). In addition, because the EDC produces extension torque about the metacarpophalangeal joints, increased EDC activity during SADD could also explain the decrease in finger torque (although the coincident increased activity of the FDI, which produces metacarpophalangeal flexion torque, would counteract this effect and may explain the smaller decrease in finger torque compared with wrist torque).

The wrist extensor muscle ECR exhibited *greater* EMG during SABD compared with SADD, demonstrating that this muscle is recruited more strongly as part of the flexion synergy than the extension synergy. This finding was interesting and unexpected, given that wrist extension is included in the clinical description of only the extension synergy. However, we found greater ECR activity during SABD than SADD in all 12 participants, which was not attributable to EMG cross-talk from other muscles based on subsequent intramuscular recordings.

While ECR's biomechanical effect is the production of wrist extension and radial deviation, it has an important stabilizing role during the production of grip. ECR counteracts the wrist flexion torque produced by the extrinsic finger flexors during gripping and places the wrist in a slightly extended position. This not only provides a more neutral wrist position, it allows the extrinsic finger flexors to operate at an optimal length for force production (Neumann et al., 2017). Therefore, co-activation of extrinsic finger flexors and ECR within the flexion synergy pattern may reflect the exposing of a latent neural circuit that supports their functional relationship within the context of grip production.

4.4. Objective 4: Comparison of flexion vs. extension synergy expression among proximal and distal joints

To compare differences in flexion and extension synergy expression among proximal and distal joints, three aspects of synergy expression were examined: (1) the relative strength of flexion vs. extension synergy expression, (2) changes in secondary torque direction due to flexion vs. extension synergy expression, and (3) the effect of overall synergy expression on flexor vs. extensor muscles.

In terms of the relative strength of synergy expression, the magnitude of flexion synergy expression was stronger than that of the extension synergy at all joints, and the difference was similar across joints. In terms of changes in secondary torque direction, there was a greater difference between the synergies at more proximal joints. Changes in secondary torque from flexion to extension at the elbow joint and from supination to pronation at the forearm were substantial (approximately half the magnitude of the change in torque direction from SABD to SADD). At the wrist and fingers, however, the changes in flexion joint torques were much smaller (approximately an eighth of the difference at the shoulder). These results suggest that the flexion and extension synergies are most strongly opposite in direction at the shoulder and become progressively more similar when moving distally along the upper limb. The clinical description of the extension synergy at the wrist–that it is variable in *direction* compared with the other joints–was supported by our results. However, the range of torque output across the flexion/extension continuum when comparing SABD and SADD torque generation was quite small.

Finally, in terms of the effect of overall synergy expression (i.e., both synergies combined) on flexor vs. extensor muscles, there was a preferential activation of flexors at both the elbow and wrist/fingers. This phenomenon was more pronounced at the more distal wrist/finger flexors by approximately two-fold across torque loads.

4.5. Neuroscientific implications

There is increasing evidence that expression of the flexion and extension synergies during voluntary movement after hemiparetic stroke is a consequence of increased recruitment of contra-lesional cortico-bulbospinal motor pathways, and that this phenomenon is proportionally related to descending motor drive requirements (Sukal et al., 2007; Ellis et al., 2012; Miller and Dewald, 2012; McPherson et al., 2018a; McPherson et al., 2018b). Based on several decades of work quantifying the progressive expression of the flexion synergy using static and dynamic paradigms (Dewald et al., 1995; Beer et al., 1999; Dewald and Beer, 2001; Beer et al., 2007; Sukal et al., 2007; Ellis et al., 2008; Ellis et al., 2009; Miller and Dewald, 2012; Lan et al., 2017a; McPherson et al., 2018a), our laboratory developed the hypothesis that when descending drive requirements are low, remaining ipsilesional corticospinal resources may be sufficient to complete a task. As descending drive requirements increase and ipsilesional motor resources are exhausted, increased use of contralesional cortico-bulbospinal motor pathways occurs as an adaptive strategy that enables motor output from the paretic limb in spite of damage to the ipsilesional corticospinal pathways. However, because bulbospinal pathways are anatomically diffuse and project to proximal and distal muscles of the upper limb, independent control of the targeted joint is compromised due to elicitation of the whole-limb flexion or extension synergy. This hypothesis is supported more directly by findings from a recent study using high density EEG (McPherson et al., 2018a), and the results of the current study are also compatible with this hypothesis.

We acknowledge that the current study provides only an indirect probe of the nervous system. However, our ability to quantify motor output and muscle activation from the whole upper limb allows for reasonable speculation about how the neuroanatomy of various bulbospinal motor pathways relates to flexion and extension synergy expression. There is more available evidence to link the flexion synergy to a specific bulbospinal pathway than there is for the extension synergy. The reticulospinal tract specifically has been implicated in underlying flexion synergy expression. In part, this is due to the similarities between the anatomy and function of the reticulospinal pathway, as demonstrated in non-human primates (Davidson and Buford, 2006; Davidson et al., 2007; Riddle et al., 2009; Herbert et al., 2010; Baker, 2011; Zaaimi et al., 2012; Baker et al., 2015). This assertion is also supported by recent findings in humans from high-resolution diffusion tensor imaging of the brainstem (Owen et al., 2017), elicitation of brainstem reflexes (Ellis et al., 2012; McPherson et al., 2018a), and neuropharmacological probes (McPherson et al., 2018b). For further discussion of the role of the reticulospinal pathways in flexion synergy expression, see Miller and Dewald (2012).

In terms of extension synergy expression, there are three neural pathways whose anatomy could reasonably provide a whole-limb extension pattern: (1) the ipsilesional reticulospinal

pathway (Davidson and Buford, 2006; Davidson et al., 2007; Herbert et al., 2010), (2) a secondary output pattern from the contralesional reticulospinal pathway that facilitates ipsilateral extensors rather than flexors (Wilson and Yoshida, 1968, 1969; Peterson, 1979; Schepens and Drew, 2004, 2006; Herbert et al., 2010), and (3) the vestibulospinal pathway (Wilson and Yoshida, 1968, 1969; Grillner et al., 1970, 1971; Matsuyama and Drew, 2000b, 2000a). (For a more extensive discussion, see Miller (2014), pg. 119.) The relative contributions of these pathways cannot be inferred with currently available evidence. Thus, additional work in animal models and in humans is necessary to investigate these possibilities further.

4.6. Implications for clinical research

Findings of the study underscore the need to incorporate whole-limb behavior when examining motor control of the paretic hand or designing rehabilitation interventions for individuals with moderate-to-severe impairment. Results from studies focusing on the hand in isolation may not generalize to functional scenarios when proximal muscles are concurrently activated.

Insight derived from previous studies quantifying flexion and extension synergy expression has provided the foundation for a novel physical therapy intervention for reaching (Ellis et al., 2008; Ellis et al., 2009; Ellis et al., 2016a; Ellis et al., 2018). Such an approach could also be applied to interventions for the hand, although the potential for regaining hand function therapeutically in patients with severe impairment is uncertain. For these individuals, the use of neuroprostheses may be necessary. While the performance of such devices during concurrent shoulder activation has been found to degrade (Lin, 2000; Chae and Hart, 2003), recent advancements that incorporate results from flexion synergy quantification improve performance during whole-limb activation (Makowski et al., 2013, 2014, 2015; Lan et al., 2017b).

As evidence for an increased influence of the reticulospinal pathway post-stroke has grown, several recent studies have suggested that this pathway a promising target for rehabilitation interventions for the arm and hand in this population (Riddle et al., 2009; Bradnam et al., 2013; Honeycutt et al., 2013; Bachmann et al., 2014; Honeycutt and Perreault, 2014; Honeycutt et al., 2015). Because the reticulospinal pathway projects throughout the arm and hand, increased excitatory synaptic input from this pathway could improve the likelihood of motoneuron depolarization and subsequent muscle activation. However, some of these studies have acknowledged that targeting the reticulospinal pathway may be less successful or not successful for individuals with severe impairment (Honeycutt and Perreault, 2014; Honeycutt et al., 2015). We suggest that a sufficient amount of residual corticospinal resources may be necessary to facilitate selective motor output by balancing the diffuse excitation provided by the reticulospinal pathway. Without enough concurrent corticospinal drive, upregulation of the reticulospinal pathway may instead reinforce the whole-limb flexion and extension synergies. Although the presence of muscle activity constrained within the flexion and extension synergies is arguably better for an individual's quality of life than having a flaccid limb, we suggest that upregulation of the reticulospinal pathway could be

contraindicated in individuals with severe motor impairment who demonstrated the synergistic movement patterns.

4.7. Limitations and future work

Several limitations to the study should be considered. First, data were collected from a relatively small sample at one point in time, and participants were in the chronic state post-stroke. Although the study did not include longitudinal measurements, results from certain aspects of the study (e.g., quantification of elbow, wrist, and finger torques during expression of the flexion synergy and quantification of elbow torques during expression of the extension synergy) repeated portions of previous studies in the literature and corroborated their findings (Dewald and Beer, 2001; Ellis et al., 2005; Miller and Dewald, 2012). Additional research is necessary to determine how expression of the flexion and extension synergies emerges during the acute and sub-acute phases.

While one selection criterion for participation in the study was moderate-to-severe motor impairment, the majority of participants we enrolled were severely impaired. It would be interesting to examine extension synergy expression in a larger cohort of participants with a wider range of impairments to explore whether the various extension synergy patterns seen could be associated with factors related to impairment or the extent of corticospinal and corticobulbar tract damage. Previous work has shown that the severity of flexion synergy expression is correlated with motor impairment within the moderate-to-severely impaired population (Ellis et al., 2008; Miller and Dewald, 2012; Lan et al., 2017a; Yao and Dewald, 2018). Recent findings from imaging studies using EEG (McPherson et al., 2018a) and diffusion tensor imaging (Owen et al., 2017) support the hypothesis that utilization of contralesional cortico-reticulospinal pathways during paretic limb movement is associated with the degree of motor impairment. Based on preliminary work in our laboratory, we hypothesize that flexion and extension synergy expression also occurs in individuals with mild impairment, but only during tasks that require high levels of descending drive.

Acknowledgments

The authors would like to acknowledge Rebecca Covode, BS for assistance with data collection and Natalia Sanchez, PhD, Meriel Owen, PhD, and Carolina Carmona, DPT for lesion location information. This work was supported by NIH grants R01HD039343 (JPAD) and T32HD057845 (JPAD), NIDILRR grant H133G070089 (JPAD) and a Promotion of Doctoral Studies II Scholarship from the Foundation for Physical Therapy Research, Inc. (LMM). Study sponsors had no role in the collection, analysis and interpretation of data and in the writing of the manuscript.

Abbreviations:

SABD	shoulder abduction
SADD	shoulder adduction
EMG	electromyography
FCR	flexor carpi radialis
FDP	flexor digitorum profundus

FDI	first dorsal interosseous
ECR	extensor carpi radialis
EDC	extensor digitorum communis
FPB	flexor pollicis brevis
EPL	extensor pollicis longus
FMA	upper extremity Fugl-Meyer Motor Assessment
CMSAh	hand portion of the Chedoke-McMaster Stroke Assessment
WFTS	Wrist and Finger Torque Sensor
BG	Basal Ganglia
TH	Thalamus
IC	Internal Capsule
CFL	Cortical Frontal Lobe
SFL	Subcortical Frontal Lobe
CPL	Cortical Parietal Lobe
CTL	Cortical Temporal Lobe
HC	Hippocampus
IN	Insula
N/A	Not Available

References

Bachmann LC, Lindau NT, Felder P, Schwab ME. Sprouting of brainstem-spinal tracts in response to unilateral motor cortex stroke in mice. J Neurosci 2014;34:3378–89. [PubMed: 24573294]

Baker SN. The primate reticulospinal tract, hand function and functional recovery. J Physiol 2011;589:5603–12. [PubMed: 21878519]

Baker SN, Zaaimi B, Fisher KM, Edgley SA, Soteropoulos DS. Pathways mediating functional recovery. Prog Brain Res 2015;218:389–412. [PubMed: 25890147]

Beer R, Dewald J, Dawson M, Rymer W. Target-dependent differences between free and constrained arm movements in chronic hemiparesis. Exp Brain Res 2004;156:458–70. [PubMed: 14968276]

Beer R, Given J, Dewald J. Task-dependent weakness at the elbow in patients with hemiparesis. Arch Phys Med Rehabil 1999;80:766–72. [PubMed: 10414760]

Beer RF, Ellis MD, Holubar BG, Dewald JP. Impact of gravity loading on post-stroke reaching and its relationship to weakness. Muscle Nerve 2007;36:242–50. [PubMed: 17486581]

Bowden JL, Taylor JL, McNulty PA. Voluntary activation is reduced in both the more and less-affected upper limbs after unilateral stroke. Front Neurol 2014;5:239. [PubMed: 25477862]

Bradnam LV, Stinear CM, Byblow WD. Ipsilateral motor pathways after stroke: implications for non-invasive brain stimulation. Front Hum Neurosci 2013;7:184. [PubMed: 23658541]

Brunnstrom S Movement therapy in hemiplegia: a neurophysiological approach. New York: Harper and Row; 1970.

Cavanagh PR, Komi PV. Electromechanical delay in human skeletal muscle under concentric and eccentric contractions. Eur J Appl Physiol Occup Physiol 1979;42:159–63. [PubMed: 527577]

Chae J, Hart R. Intramuscular hand neuroprosthesis for chronic stroke survivors. Neurorehabil Neural Repair 2003;17:109–17. [PubMed: 12814056]

Colebatch JG, Gandevia SC. The distribution of muscular weakness in upper motor neuron lesions affecting the arm. Brain 1989;112:749–63. [PubMed: 2731028]

Davidson AG, Buford JA. Bilateral actions of the reticulospinal tract on arm and shoulder muscles in the monkey: stimulus triggered averaging. Exp Brain Res 2006;173:25–39. [PubMed: 16506008]

Davidson AG, Schieber MH, Buford JA. Bilateral spike-triggered average effects in arm and shoulder muscles from the monkey pontomedullary reticular formation. J Neurosci 2007;27:8053–8. [PubMed: 17652596]

Dewald J, Beer R. Abnormal joint torque patterns in the paretic upper limb of subjects with hemiparesis. Muscle Nerve 2001;24:273–83. [PubMed: 11180211]

Dewald J, Pope S, Given J, Buchanan T, Rymer W. Abnormal muscle coactivation patterns during isometric torque generation at the elbow and shoulder in hemiparetic subjects. Brain 1995;118:495–510. [PubMed: 7735890]

Ellis MD, Acosta AM, Yao J, Dewald JP. Position-dependent torque coupling and associated muscle activation in the hemiparetic upper extremity. Exp Brain Res 2007;176:594–602. [PubMed: 16924488]

Ellis MD, Carmona C, Drogos J, Dewald JPA. Progressive abduction loading therapy with horizontal-plane viscous resistance targeting weakness and flexion synergy to treat upper limb function in chronic hemiparetic stroke: a randomized clinical trial. Front Neurol 2018;9:71. [PubMed: 29515514]

Ellis MD, Carmona C, Drogos J, Traxel S, Dewald JP. Progressive abduction loading therapy targeting flexion synergy to regain reaching function in chronic stroke: Preliminary results from an RCT. In: Conf Proc IEEE Eng Med Biol Soc. p. 5837–40.

Ellis MD, Drogos J, Carmona C, Keller T, Dewald JP. Neck rotation modulates flexion synergy torques indicating an ipsilateral reticulospinal source for impairment in stroke. J Neurophysiol 2012;108:3096–104. [PubMed: 22956793]

Ellis MD, Holubar BG, Acosta AM, Beer RF, Dewald JP. Modifiability of abnormal isometric elbow and shoulder joint torque coupling after stroke. Muscle Nerve 2005;32:170–8. [PubMed: 15880629]

Ellis MD, Lan Y, Yao J, Dewald JP. Robotic quantification of upper extremity loss of independent joint control or flexion synergy in individuals with hemiparetic stroke: a review of paradigms addressing the effects of shoulder abduction loading. J Neuroeng Rehabil 2016b;13:95. [PubMed: 27794362]

Ellis MD, Schut I, Dewald JPA. Flexion synergy overshadows flexor spasticity during reaching in chronic moderate to severe hemiparetic stroke. Clin Neurophysiol 2017;128:1308–14. [PubMed: 28558314]

Ellis MD, Sukal T, DeMott T, Dewald JP. Augmenting clinical evaluation of hemiparetic arm movement with a laboratory-based quantitative measurement of kinematics as a function of limb loading. Neurorehabil Neural Repair 2008;22:321–9. [PubMed: 18326888]

Ellis MD, Sukal-Moulton T, Dewald JP. Progressive shoulder abduction loading is a crucial element of arm rehabilitation in chronic stroke. Neurorehabil Neural Repair 2009;23:862–9. [PubMed: 19454622]

Fugl-Meyer A, Jaasko L, Leyman I, Olsson S, Steglind S. The post-stroke hemiplegic patient. 1. A method for evaluation of physical performance. Scand J Rehabil Med 1975;7:13–31. [PubMed: 1135616]

Gonzalez RV, Buchanan TS, Delp SL. How muscle architecture and moment arms affect wrist flexion-extension moments. J Biomech 1997;30:705–12. [PubMed: 9239550]

Gowland C, Van Hullenaar S, Torresin W, Moreland J, Vanspall B, Barreca S, et al. Chedoke-McMaster Stroke Assessment: development, validation, and administration manual. Hamilton: Chedoke-McMaster Hospitals and McMaster University; 1995.

Grillner S, Hongo T, Lund S. The vestibulospinal tract. Effects on alpha-motoneurones in the lumbosacral spinal cord in the cat. Exp Brain Res 1970;10:94–120. [PubMed: 5411977]

Grillner S, Hongo T, Lund S. Convergent effects on alpha motoneurones from the vestibulospinal tract and a pathway descending in the medial longitudinal fasciculus. Exp Brain Res 1971;12:457–79. [PubMed: 5093725]

Herbert WJ, Davidson AG, Buford JA. Measuring the motor output of the pontomedullary reticular formation in the monkey: do stimulus-triggered averaging and stimulus trains produce comparable results in the upper limbs? Exp Brain Res 2010;203:271–83. [PubMed: 20379705]

Honeycutt CF, Kharouta M, Perreault EJ. Evidence for reticulospinal contributions to coordinated finger movements in humans. J Neurophysiol 2013;110:1476–83. [PubMed: 23825395]

Honeycutt CF, Perreault EJ. Deficits in startle-evoked arm movements increase with impairment following stroke. Clin Neurophysiol 2014;125:1682–8. [PubMed: 24411525]

Honeycutt CF, Tresch UA, Perreault EJ. Startling acoustic stimuli can evoke fast hand extension movements in stroke survivors. Clin Neurophysiol 2015;126: 160–4. [PubMed: 25002367]

Kamper DG, Fischer HC, Cruz EG, Rymer WZ. Weakness is the primary contributor to finger impairment in chronic stroke. Arch Phys Med Rehabil 2006; 87:1262–9. [PubMed: 16935065]

Kamper DG, Harvey R, Suresh S, Rymer WZ. Relative contributions of neural mechanisms versus muscle mechanics in promoting finger extension deficits following stroke. Muscle Nerve 2003;28:309–18. [PubMed: 12929190]

Lan Y, Yao J, Dewald JPA. The impact of shoulder abduction loading on volitional hand opening and grasping in chronic hemiparetic stroke. Neurorehabil Neural Repair 2017a;31:521–9. [PubMed: 28506146]

Lan Y, Yao J, Dewald JPA. Reducing the impact of shoulder abduction loading on the classification of hand opening and grasping in individuals with poststroke flexion synergy. Front Bioeng Biotechnol 2017b;5:39. [PubMed: 28713811]

Lin C The effects of ipsilateral forearm movement and contralateral hand grasp on the spastic hand opened by electrical stimulation. Neurorehabil Neural Repair 2000;14:199–205. [PubMed: 11272476]

Makowski NS, Knutson JS, Chae J, Crago PE. Interaction of poststroke voluntary effort and functional neuromuscular electrical stimulation. J Rehabil Res Dev 2013;50:85–98. [PubMed: 23516086]

Makowski NS, Knutson JS, Chae J, Crago PE. Functional electrical stimulation to augment poststroke reach and hand opening in the presence of voluntary effort: a pilot study. Neurorehabil Neural Repair 2014;28:241–9. [PubMed: 24270058]

Makowski NS, Knutson JS, Chae J, Crago PE. Control of robotic assistance using poststroke residual voluntary effort. IEEE Trans Neural Syst Rehabil Eng 2015;23:221–31. [PubMed: 25373107]

Matsuyama K, Drew T. Vestibulospinal and reticulospinal neuronal activity during locomotion in the intact cat. I. Walking on a level surface. J Neurophysiol 2000a;84:2237–56. [PubMed: 11067969]

Matsuyama K, Drew T. Vestibulospinal and reticulospinal neuronal activity during locomotion in the intact cat. II. Walking on an inclined plane. J Neurophysiol 2000b;84:2257–76. [PubMed: 11067970]

McNulty PA, Lin G, Doust CG. Single motor unit firing rate after stroke is higher on the less-affected side during stable low-level voluntary contractions. Front Hum Neurosci 2014;8:518. [PubMed: 25100969]

McPherson JG, Chen A, Ellis MD, Yao J, Heckman CJ, Dewald JP. Progressive recruitment of contralesional cortico-reticulospinal pathways drives motor impairment post-stroke. J Physiol 2018a;596:1211–25. [PubMed: 29457651]

McPherson JG, Ellis MD, Harden RN, Carmona C, Drogos JM, Heckman CJ, et al. Neuromodulatory inputs to motoneurons contribute to the loss of independent joint control in chronic moderate to severe hemiparetic stroke. Front Neurol 2018b;9:470. [PubMed: 29977224]

McPherson JG, Stienen AH, Drogos JM, Dewald JP. Modification of spastic stretch reflexes at the elbow by flexion synergy expression in individuals with chronic hemiparetic stroke. Arch Phys Med Rehabil 2018c;99:491–500. [PubMed: 28751255]

Miller LC. Quantification of abnormal coupling between the paretic upper arm and hand of individuals with chronic hemiparetic stroke using neurophysiological and biomechanical measurements (Doctoral dissertation). ProQuest Dissertations and Theses, No. 3669288. Northwestern University; 2014.

Miller LC, Dewald JP. Involuntary paretic wrist/finger flexion forces and EMG increase with shoulder abduction load in individuals with chronic stroke. Clin Neurophysiol 2012;123:1216–25. [PubMed: 22364723]

Miller LC, Thompson CK, Negro F, Heckman CJ, Farina D, Dewald JPA. High-density surface EMG decomposition allows for recording of motor unit discharge from proximal and distal flexion synergy muscles simultaneously in individuals with stroke. In: Conf Proc IEEE Eng Med Biol Soc.. p. 5340–4.

Neumann DA, Kelly ER, Kiefer CL, Martens K, Grosz CM. Kinesiology of the musculoskeletal system: foundations for rehabilitation. 3rd ed St. Louis, Missouri: Elsevier; 2017.

Owen M, Ingo C, Dewald JPA. Upper extremity motor impairments and microstructural changes in bulbospinal pathways in chronic hemiparetic stroke. Front Neurol 2017;8:257. [PubMed: 28659855]

Perotto A, Delagi EF. Anatomical guide for the electromyographer: the limbs and trunk. 3rd ed Springfield, IL, USA: Charles C. Thomas; 1994.

Peterson BW. Reticulospinal projections to spinal motor nuclei. Annu Rev Physiol 1979;41:127–40. [PubMed: 373586]

Radomski MV, Latham CAT. Occupational therapy for physical dysfunction. 6th ed Philadelphia: Lippincott Williams & Wilkins; 2008.

Riddle CN, Edgley SA, Baker SN. Direct and indirect connections with upper limb motoneurons from the primate reticulospinal tract. J Neurosci 2009;29:4993–9. [PubMed: 19369568]

Schepens B, Drew T. Independent and convergent signals from the pontomedullary reticular formation contribute to the control of posture and movement during reaching in the cat. J Neurophysiol 2004;92:2217–38. [PubMed: 15175364]

Schepens B, Drew T. Descending signals from the pontomedullary reticular formation are bilateral, asymmetric, and gated during reaching movements in the cat. J Neurophysiol 2006;96:2229–52. [PubMed: 16837662]

Seo NJ, Rymer WZ, Kamper DG. Delays in grip initiation and termination in persons with stroke: effects of arm support and active muscle stretch exercise. J Neurophysiol 2009;101:3108–15. [PubMed: 19357330]

Stienen AH, Moulton TS, Miller LC, Dewald JP. Wrist and Finger Torque Sensor for the quantification of upper limb motor impairments following brain injury. In: IEEE Int Conf Rehabil Robot. 2011 p. 5975464.

Sukal T, Ellis M, Dewald J. Shoulder abduction-induced reductions in reaching work area following hemiparetic stroke: neuroscientific implications. Exp Brain Res 2007;176:594–602. [PubMed: 16924488]

Turton A, Wroe S, Trepte N, Fraser C, Lemon RN. Contralateral and ipsilateral EMG responses to transcranial magnetic stimulation during recovery of arm and hand function after stroke. Electroencephalogr Clin Neurophysiol 1996;101:316–28. [PubMed: 8761041]

Twitchell TE. The restoration of motor function following hemiplegia in man. Brain 1951;74:443–80. [PubMed: 14895765]

Wilkins KB, Owen M, Ingo C, Carmona C, Dewald JPA, Yao J. Neural plasticity in moderate to severe chronic stroke following a device-assisted task-specific arm/hand intervention. Front Neurol 2017;8:284. [PubMed: 28659863]

Wilson VJ, Yoshida M. Vestibulospinal and reticulospinal effects on hindlimb, forelimb, and neck alpha motoneurons of the cat. Proc Natl Acad Sci U S A 1968;60:836–40. [PubMed: 5243926]

Wilson VJ, Yoshida M. Comparison of effects of stimulation of Deiters' nucleus and medial longitudinal fasciculus on neck, forelimb, and hindlimb motoneurons. J Neurophysiol 1969;32:743–58. [PubMed: 4309026]

Yao J, Dewald JPA. The increase in overlap of cortical activity preceding static elbow/shoulder motor tasks is associated with limb synergies in severe stroke. Neurorehabil Neural Repair 2018 1545968318781028.

Zaaimi B, Edgley SA, Soteropoulos DS, Baker SN. Changes in descending motor pathway connectivity after corticospinal tract lesion in macaque monkey. Brain 2012;135:2277–89. [PubMed: 22581799]

HIGHLIGHTS

- The post-stroke flexion and extension synergies were quantified at proximal and distal arm joints.
- Flexion and extension synergy expression throughout the arm increased with shoulder torque level.
- The synergies were similar at the wrist and fingers, but opposite at the elbow.

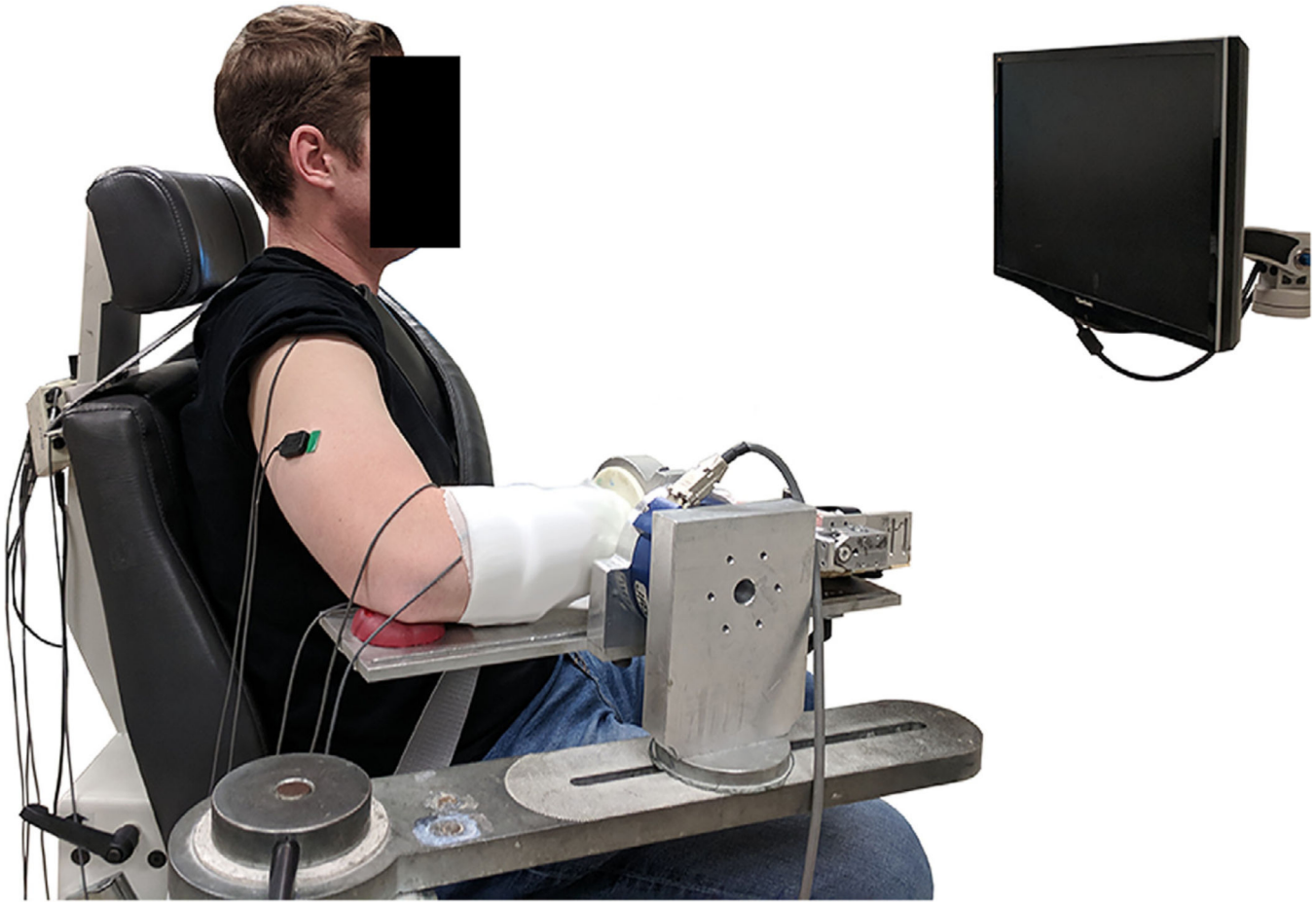

Fig. 1.

Isometric testing device to measure shoulder, elbow, wrist and finger torques. Real-time visual feedback of torque magnitude in the desired degree-of-freedom is displayed on a computer monitor. The red support cushion on the elbow was positioned for participant comfort during setup and rest breaks but was removed for data collection. (For interpretation of the references to colour in this figure legend, the reader is referred to the web version of this article.)

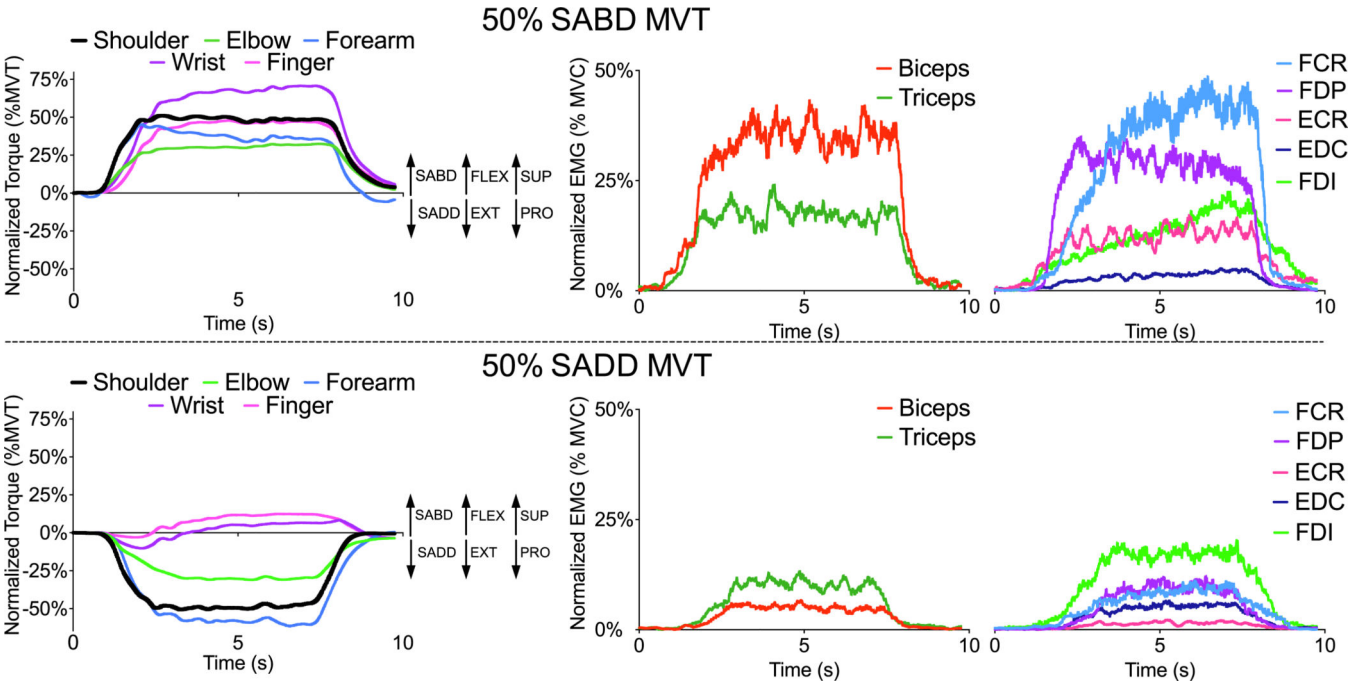

Fig. 2.

Representative paretic torque (left panel) and EMG (middle and right panel) traces from a single trial of 50% SABD MVT (top panel) and 50% SADD MVT (bottom panel) from the same participant. Sign conventions for the joint torques are shown with arrows. Elbow EMG data are shown in the middle panel (biceps, triceps) and wrist and finger EMG data are shown in the right panel (FCR, FDP, ECR, EDC, FDI). Thumb muscles are not shown for brevity.

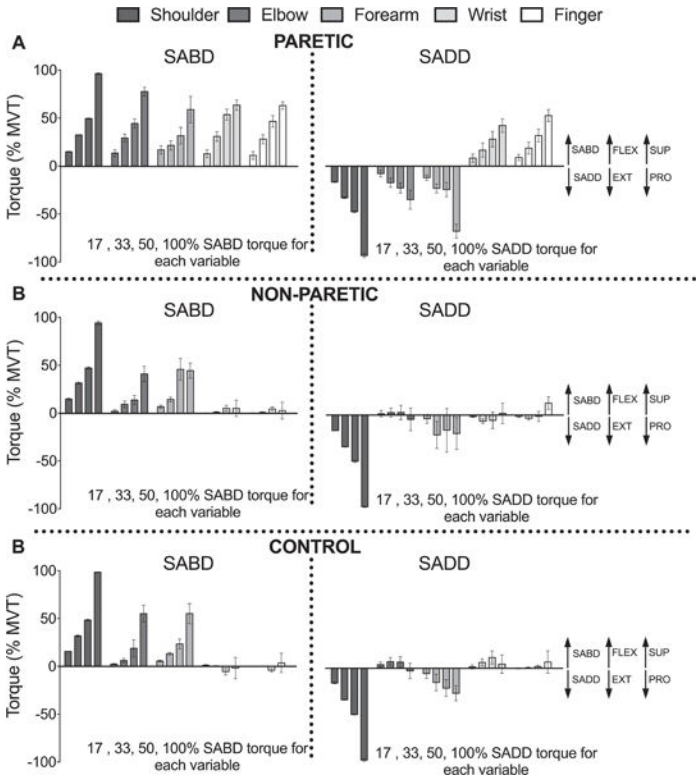

Fig. 3.

Paretic, non-paretic, and control torque results from the shoulder, elbow, forearm, wrist and finger joints. Group mean ± SEM shoulder abduction (+)/adduction (−), elbow flexion (+)/extension (−), forearm supination (+)/pronation (−), wrist flexion (+)/extension (−), and finger flexion (+)/extension (−) torques produced during the generation of 17, 33, 50, and 100% MVT of SABD torque (left panels) or 17, 33, 50, and 100% MVT of SADD torque (right panels), in the paretic (A), non-paretic (B), and control (C) limbs.

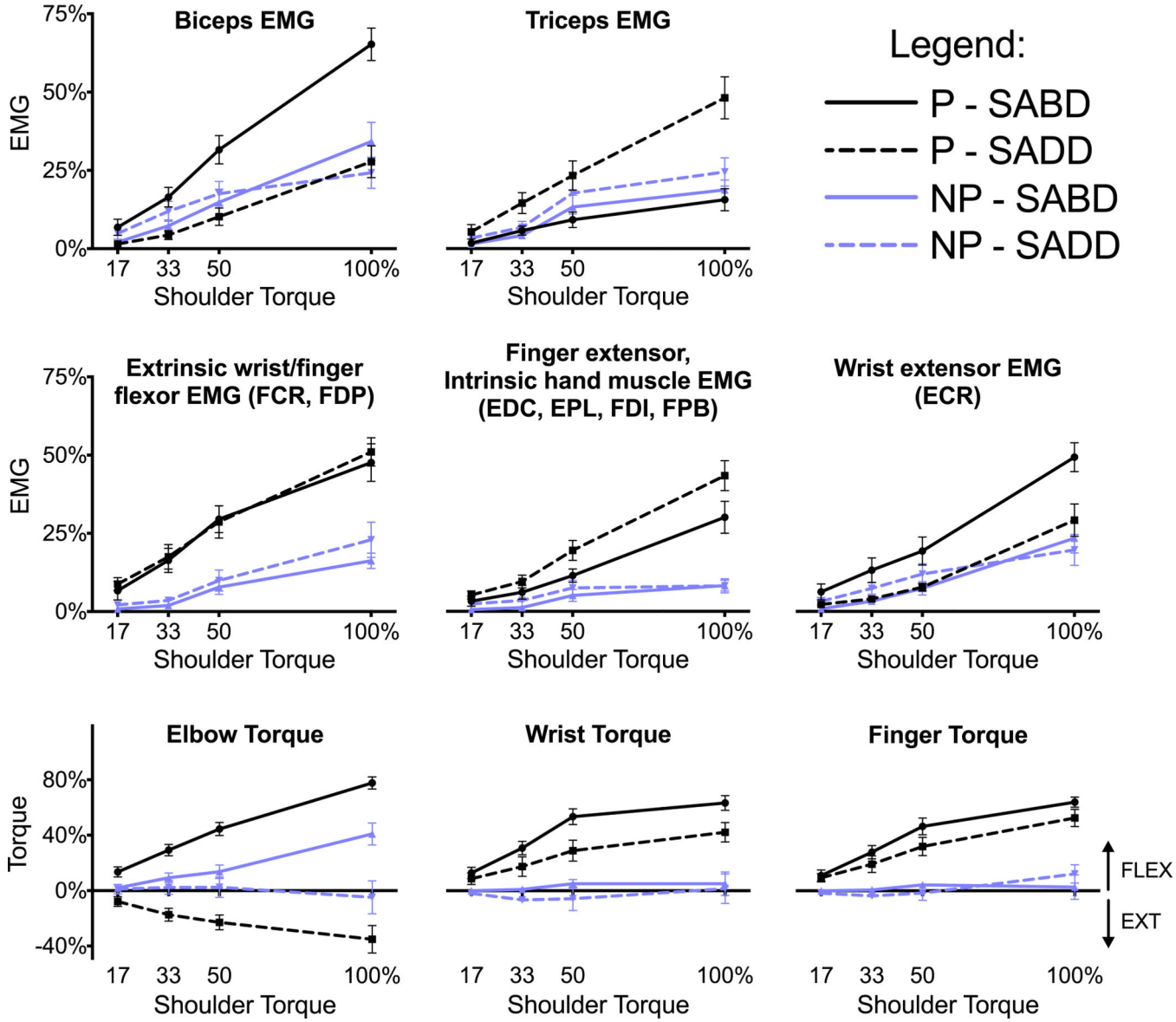

Fig. 4.

Paretic (black) and non-paretic (light purple) EMG from elbow, wrist, and finger muscles. Group mean ± SEM biceps, triceps, extrinsic wrist/finger flexor, wrist/finger extensor/intrinsic hand muscle, and wrist extensor EMG generated during 17, 33, 50, and 100% MVT of SABD torque (solid lines) or 17, 33, 50, and 100% MVT of SADD torque (dashed lines). Elbow, wrist, and finger torques from the left panel of Fig. 3A and B are displayed again as line graphs for reference (positive values denote flexion torques; negative values denote extension torques). (For interpretation of the references to colour in this figure legend, the reader is referred to the web version of this article.)

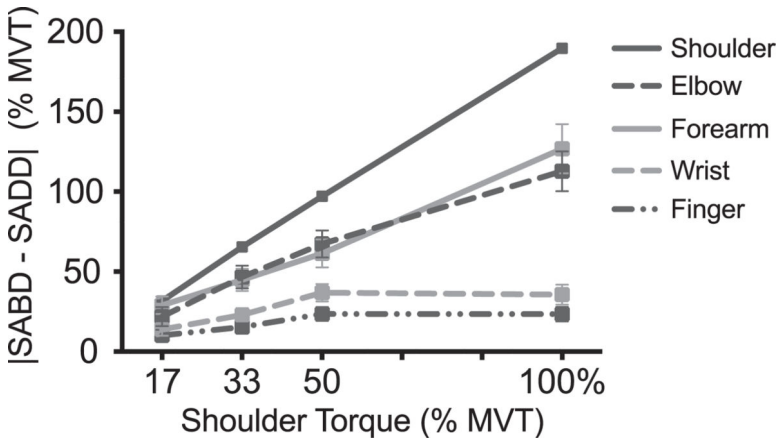

Fig. 5.

Magnitude of the change in direction of secondary torques from SABD to SADD torque generation at the paretic elbow, forearm, wrist and finger joints. Values for shoulder torque (i.e., primary torque) are shown in solid black for comparison. Group mean ± SEM values during shoulder torque generation at 17, 33, 50, and 100% MVT are shown. On average across torque load, values for the shoulder were significantly higher than those of each other joints, and values for the elbow and forearm joints were significantly higher than those for the wrist and fingers.

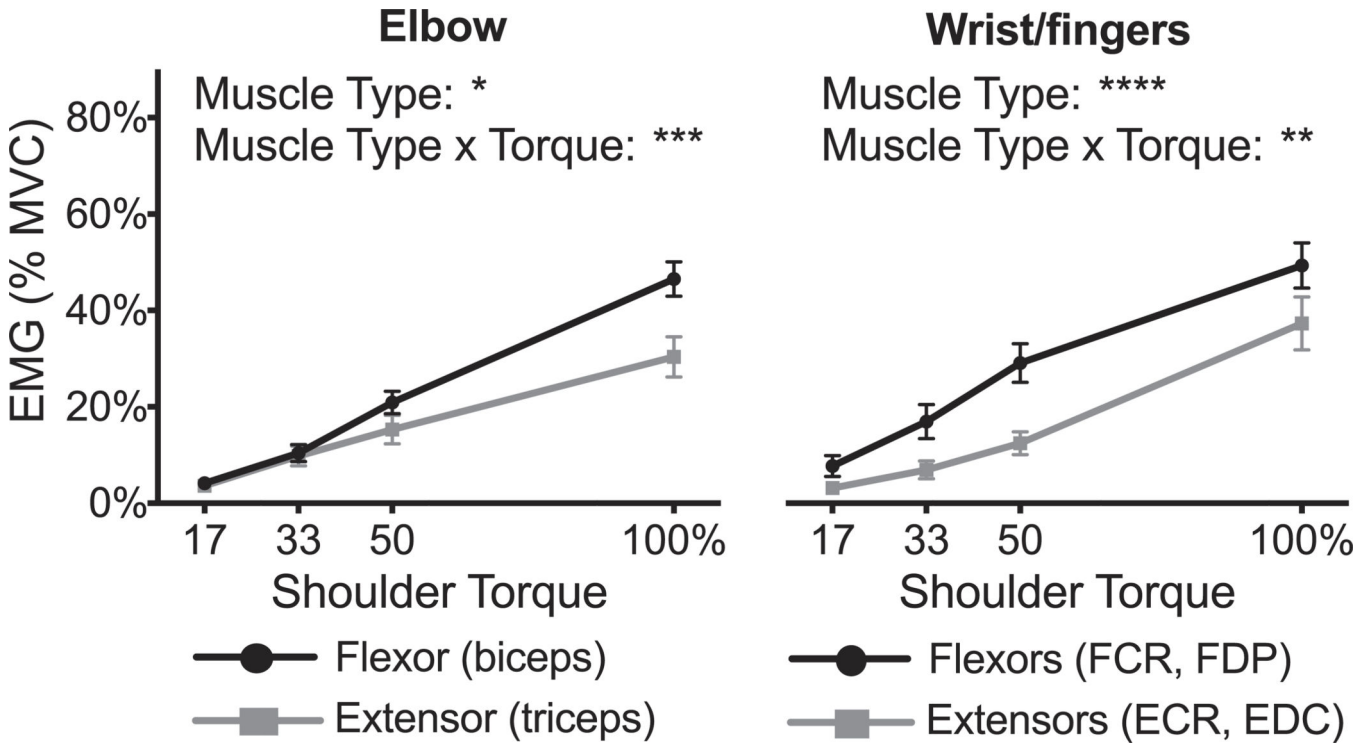

Fig. 6.

Paretic group mean ± SEM flexor (black) and extensor (grey) EMG data for elbow muscles (left plot) and extrinsic wrist/finger muscles (right plot). Values represent an average of SABD and SADD torque generation conditions for four levels of torque (17, 33, 50, 100% MVT). Flexors are recruited to a greater extent than extensors for both the elbow and wrist/finger joints. ANOVA results are displayed in each subplot for the main effect of muscle type (flexor, extensor) and the interaction of muscle type-by-torque load. Significant results are indicated by * ($p < 0.05$), ** ($p < 0.01$), *** ($p < 0.001$), and **** ($p < 0.0001$).

Table 1

Demographics of the participants with chronic hemiparetic stroke.

Participant	Age	Sex	Affected/dominant	Lesion location	Years post-stroke	FMA	CMSAh
1	60	F	R/R	BG, TH, IC	26.6	20	3
2	70	M	L/L	N/A	11.4	24	2
3	63	M	R/R	BG, IC, CFL, SFL, IN	4.5	13	3
4	60	F	R/R	BG, IC, TH, HC	5.3	30	3
5	59	M	L/L	IC	3.8	25	4
6	57	M	L/R	BG, IC	6.5	24	3
7	56	F	L/R	N/A	9.0	15	3
8	67	M	R/L	BG, TH, IC, CTL	17.0	19	2
9	47	M	R/L	N/A	25.5	26	3
10	54	M	L/L	CPL, CTL, CFL	5.6	31	3
11	55	M	R/L	IC	5.1	20	4
12	55	M	R/R	IC	3.5	29	3
Mean (SD)	**59.0 (6.2)**				**10.3 (8.3)**	**22.7 (5.9)**	**3.0 (0.6)**

FMA = Upper extremity score of the Fugl-Meyer Motor Assessment (max = 66); CMSAh = Hand portion of the Chedoke-McMaster Stroke Assessment (max = 7); BG = Basal Ganglia; TH = Thalamus; IC = Internal Capsule; CFL = Cortical Frontal Lobe; SFL = Subcortical Frontal Lobe; CPL = Cortical Parietal Lobe; CTL = Cortical Temporal Lobe; HC = Hippocampus; IN = Insula; N/A = Not Available.

Table 2

Between-limb results for torque variables during SABD (Obj. 1) and during SADD (Obj. 2).

Task:	***Obj. 1:* SABD**		***Obj. 2:* SADD**	
ANOVA effect	**Limb**	**Limb by torque load**	**Limb**	**Limb by torque load**
Torque variable				
Elbow	***	***	**	*ns*
Forearm	*ns*	*ns*	*ns +*	***
Wrist	****	****	***	*
Finger	****	****	***	*

Results of separate 2 × 4 (limb by torque load) repeated measures ANOVAs for each torque variable and shoulder direction.

Asterisks indicate significant differences at

(*) $p < 0.05$

(**) $p < 0.01$ or

(****) $p < 0.0001$

ns + indicates $0.05 < p < 0.10$ and *ns* indicates $p > 0.1$ (exact p-values for $p > 0.05$ are referenced in the text).

Clin Neurophysiol. Author manuscript; available in PMC 2021 February 03.

Table 3

Between-limb results for EMG variables during SABD (Obj. 1) and during SADD (Obj. 2).

Task:	***Obj. 1:* SABD**		***Obj. 2:* SADD**	
ANOVA effect	**Limb**	**Limb by torque load**	**Limb**	**Limb by torque load**
EMG variable				
Biceps	**	***	*ns*	*ns*
Triceps	*ns*	*ns*	*ns +*	**
Extrinsic wrist/finger flexors	****	****	***	**
Wrist/finger extensors, intrinsic hand muscles	***	****	***	****
ECR	**	***	*ns*	*ns +*

Results of separate 2 × 4 (limb by torque load) repeated measures ANOVAs for each EMG variable and shoulder direction.

Asterisks indicate significant differences at

$^{(*)}p < 0.05$

$^{(**)}p < 0.01$ or

$^{(****)}p < 0.0001$

ns + indicates $0.05 < p < 0.10$ and *ns* indicates $p > 0.1$ (exact p-values for $p > 0.05$ are referenced in the text).

Table 4

Within-limb results for torque variables: effect of shoulder direction and torque load.

Limb:	***Paretic limb***		***Non-paretic limb***	
ANOVA effect	**Shoulder direction**	**Shoulder direction by torque load**	**Shoulder direction**	**Shoulder direction by torque load**
Torque variable				
Elbow	****	****	*	*ns*
Forearm	****	****	****	***
Wrist	*ns* +	*	*ns*	*ns*
Finger	*ns* +	*ns*	*ns*	*ns*

Results of separate 2 × 4 (shoulder direction by torque load) repeated measures ANOVAs for each torque variable and limb.

Asterisks indicate significant effects at

(*) $p < 0.05$

(**) $p < 0.01$ and

(****) $p < 0.0001$.

ns + indicates $0.05 < p < 0.10$ and *ns* indicates $p > 0.1$ (exact p-values for $p > 0.05$ are referenced in the text).

Table 5

Within-limb results for EMG variables: effect of shoulder direction and torque load.

Limb:	***Paretic limb***		***Non-paretic limb***	
ANOVA effect	**Shoulder direction**	**Shoulder direction by torque load**	**Shoulder direction**	**Shoulder direction by torque load**
EMG variable				
Biceps	***	****	*ns*	*ns*
Triceps	**	****	*ns* +	*ns*
Extrinsic wrist/finger flexors	*ns*	*ns*	*ns*	*ns*
Wrist/finger extensors, intrinsic hand muscles	*	**	*ns*	*ns*
ECR	**	**	*ns*	*ns*

Results of separate 2 × 4 (shoulder direction by torque load) repeated measures ANOVAs for each EMG variable and limb.

Asterisks indicate significant effects at

$^{(*)}p < 0.05$

$^{(**)}p < 0.01$

$^{(***)}p < 0.001$ and

$^{(****)}p < 0.0001$.

ns + indicates $0.05 < p < 0.10$ and *ns* indicates $p > 0.1$ (exact *p*-values for $p > 0.05$ are referenced in the text).